Conformational Contraction and Hydrolysis of Hyaluronate in Sodium Hydroxide Solutions

Snehasish Ghosh, Ivan Kobal,† Dino Zanette,‡ and Wayne F. Reed*

Department of Physics, Tulane University, New Orleans, Louisiana 70118

Received July 13, 1992; Revised Manuscript Received April 28, 1993

ABSTRACT: The effects of NaOH on the conformations, interactions, diffusion, and hydrolysis rates of hyaluronate (HA) were characterized in detail using static light scattering (i) in the traditional "batch" mode (for conformations and interactions), (ii) in a time-dependent, simultaneous multiangle mode (for the hydrolysis rates), and (iii) coupled to HPLC for preliminary characterization of distributions of hydrolysis fragments. Strikingly, the conformations, interactions, and hydrolysis rates all seem to be controlled by the titration of the HA hydroxyl groups by NaOH to yield $-O^-$, which (i) destroys single strand hydrogen bonds, leading to the very rapid destiffening and contraction of the HA coil and to a large decrease in intermolecular interactions, and (ii) leads to the slow intramolecular cleavage (hydrolysis) of glycosidic bonds. Remarkably, the root mean square radius of gyration R_g, the second virial coefficient A_2, and hydrolysis rates all appear as mutually superposing titration curves which yield a pK of around 13. Interestingly, in contrast to classical "non-draining" coil molecules, the hydrodynamic radius of HA, as measured by dynamic light scattering, is independent of [NaOH] and the contraction of R_g.

Introduction

The current report on the use of time-dependent total intensity light scattering, as well as standard static and dynamic light scattering, for the characterization of hyaluronate (HA) behavior with the concentration of sodium hydroxide NaOH, has two chief goals: First, to characterize the effect of NaOH on HA conformation, interactions, and diffusion. Second, to measure base catalyzed hydrolysis rates of HA and to make possible deductions concerning the hydrolysis mechanism and the structure of HA. Additionally, we seek to extend the recently developed theory and application of time-dependent total intensity light scattering for determining depolymerization kinetics[1-3] to simultaneous multiangle measurements. Also, the hydrolysis fragment distributions are to be monitored in a preliminary fashion using HPLC coupled to multiangle light scattering.

Our original interest in the effects of NaOH on HA was to ascertain the rates of hydrolysis which might run concurrently to a deacetylation on the acetamido moiety on the *N*-acetylglucosamine monomer, which was to be marked with a fluorescent probe.

The behavior of the hydrolysis rates as a function of NaOH concentration implicates an intramolecularly catalyzed glycosidic bond cleavage, that is, a neighboring group participation, as will be shown. Furthermore, the large contraction in HA root mean square gyration radius R_g (used as a shorthand notation for what is often represented as $\langle S^2\rangle^{1/2}$), and reduction of A_2 at high pH, further support earlier evidence that at intermediate pH ranges HA has some degree of stiffening due to local hydrogen bonded helical structure.[4-6] Much smaller decreases in R_g and A_2 are found as ionic strength C_s is increased by addition of a simple salt, such as NaCl.

The first applications of the theory of time-dependent total light scattering intensity changes for coil molecules undergoing random scission were performed on HA at a single, fixed angle using HCl[1] and hyaluronidase[3] as the depolymerizing agents. In this work data collection and analysis software were developed for a multiangle Wyatt Technology Dawn scattering photometer operating in the "batch mode", that is, with a 25 mm diameter scintillation vial instead of the HPLC flow cell. The ability to simultaneously monitor many (15) angles allows not only the average number of polymer links broken per original molecule per unit time to be determined but also the weight average molecular weight, M_w, and z-averaged mean square radius of gyration $\langle S^2\rangle_z$.

HPLC coupled to the static light scattering capabilities of the Wyatt Dawn photometer is then used for a tentative analysis of initial polydispersity of the HA and the hydrolysis fragment distributions.

Summary of Light Scattering Theory of Random Polymer Scission. A recent paper[1] showed that the random scission of an initially monodisperse population of random coils has the remarkable property of preserving the functional form of the scattering form factor $P(u)$ for ideal random coils, which has the well-known expression (Debye function)

$$P(u) = \frac{2}{u^2}(e^{-u} + u - 1) \tag{1}$$

where originally $u = q^2\langle S^2\rangle$. Here $q = (4\pi n/\lambda)\sin(\theta/2)$, $\langle S^2\rangle$ is the mean square radius of gyration of the coils of the initial monodisperse population, λ is the wavelength of the incident light, n is the index of refraction of the solvent, and θ is the scattering observation angle. If an average number of random cuts, r, is made per polymer molecule in an initially monodisperse population of random coils, then the scattering form factor is still given by eq 1, where the argument u, is now given by $u = [r + u_0]$ where $u_0 \equiv q^2\langle S^2\rangle_0$, $\langle S^2\rangle_0$ being the mean square radius of gyration of the coils before digestion begins.

Random scission of bonds means that all bonds have an equal probability of being cut when one cut is made in the entire population. The expected rate of average cuts per original molecule per time t, $\dot{r}(M,t)$ is proportional to that molecule's original weight

$$\dot{r}(M,t) = \dot{\beta}\, M \tag{2}$$

Here $\dot{\beta}$ is a rate constant expressed as number of cuts per unit time per unit mass of polymer. Experimental determination of $\dot{\beta}$ allows the initial velocity in molar bonds

* To whom correspondence should be addressed.
† On leave from J. Stefan Institute, P.O. 100, 61111 Llubljana, Slovenia.
‡ Chemistry Dept., Uni. Federal de Sta. Catarina, Florianopolis, Brasil.

0024-9297/93/2226-4685$04.00/0

broken per second to be expressed as

$$v = \dot{\beta}c \tag{3}$$

where the polymer concentration c is here expressed in mg/mL.

It has been shown in refs 2 and 3 that if $u(M,r)$ is large for all M, i.e. $q^2\langle S^2\rangle_0 > 3$ for all M in the initial mass distribution, then accurate depolymerization rate constants $\dot{\beta}$ can be determined, under the assumption of ideal coils, without knowing the polymer's initial molecular weight distribution, radii of gyration, or A_2. It suffices to measure the absolute scattering intensity (Rayleigh ratio) as a function of time $I(t)$, to determine the depolymerization kinetics. Assuming that A_2 is independent of mass (i.e. does not change, at least during the initial phase of depolymerization)[2,3]

$$\dot{\beta} = 2Kc\frac{\mathrm{d}[1/I(t)]}{\mathrm{d}t} \tag{4}$$

K is a cluster of constants given, for vertically polarized incident light, by

$$K = \frac{4\pi^2 n^2(\mathrm{d}n/\mathrm{d}c)^2}{\lambda^4 N_A} \tag{5}$$

where N_A is Avogadro's number and $\mathrm{d}n/\mathrm{d}c$ is the differential index of refraction of the solvent/polymer system.

The limiting case of eq 4 can also be reached by random coils of *any* initial size and range of u_0 if the light scattering measurements during digestion are carried out long enough to reach high values of r (and hence u) and the majority of the weight fraction of fragments can still be considered as coils.

Although u_0 can be small for HA when contracted in NaOH solution and measured at small angles, we determine rate constants in this work from high enough angles that the approximation of eq 4 is still fairly good. For example, for $\lambda = 6320$ Å at $\theta = 120°$, $u_0 = 3.35$ for HA of $R_g = 800$ Å. Problems of interpretation due to initial polydispersity are substantially reduced in this fashion.

Reference 1 showed that the number distribution of fragments after an average of r random cuts per initial polymer for an initially monodisperse population of coils is given by

$$f(r,x) = e^{-r}\delta(x-1) + e^{-rx}(r^2 - r^2x + 2r) \tag{6a}$$

The $e^{-r}\delta(x-1)$ represents the fraction of the original uncut chains that remains after r cuts. Here, $x = M/M_0$, where M_0 is the original mass of the monodisperse polymers, and $M < M_0$ is the size of a fragment. The concentration (or weight) fraction of fragments is simply

$$c(r,x) = xf(r,x) \tag{6b}$$

The number, weight, and z averages of the polymer population (M_n, M_w, and M_z, respectively) after r cuts can be found from $f(r,x)$ to be

$$M_n = M_0/(1+r) \tag{7}$$

$$M_w = M_0(2/r^2)(e^{-r} - 1 + r) \tag{8}$$

$$M_z = \frac{3M_0\left[\frac{2}{r}(e^{-r}-1) + 1 + e^{-r}\right]}{r\left[\frac{e^{-r}}{r} + 1 - 1/r\right]} \tag{9}$$

If the polymer is initially polydisperse, the fragment distribution as digestion proceeds will be modified.[2] Since the initial polydispersity of the HA was difficult to determine, the above formulas for initially monodisperse populations are used for simplicity, and the results will be seen to be good.

The effects of excluded volume, non-Gaussian behavior and mass-dependent A_2 values have been discussed and analyzed in refs 2 and 3. The conclusion in ref 3 is that ignoring non-Gaussian behavior of the coils can lead to underestimates of rate constants on the order of roughly 10% to 20% for a molecule such as HA. Recently, Monte Carlo simulations of polyelectrolyte scattering properties, however, indicate that such errors due to ignoring excluded volume may be even smaller than the estimates in ref 3 and that experimentally measuring such differences may be extremely difficult for single wavelength light scattering experiments.[7] We do not pursue such corrections or analyses in this work.

Materials and Methods

Materials. Bacterial hyaluronate from *Streptococcus zooepidemicus* was obtained from Sigma (sodium salt form) and used without further purification. The protein and sulfated glycosaminoglycan assays and the methodologies used for this material have been previously reported.[3,8,9]

Unless otherwise stated, all stock solutions of HA were made at 1 mg/mL in unbuffered 150 mM NaCl solutions. These solutions were slowly stirred for at least 2 days before use.

For determination of hydrolysis rates equal amounts of the 1 mg/mL HA stock at 150 mM NaCl and the appropriate strength NaOH stock were mixed together. For determination of R_g, A_2, and diffusion coefficients, 0.25 mg/mL HA solutions at 150 mM NaCl were serially titrated with stocks of NaOH (and for certain experiments, with NaCl). All samples for light scattering studies were filtered through 0.22 μM Triton-free mixed ester cellulose filters obtained from Millipore (Milex-GS series).

All concentrations used were those of the weighed product directly from the bottle. A determination of water content of the powder using a thermal balance showed 5% water by weight several days after opening a bottle of HA, reclosing, and storing in a freezer. A slight overestimation of hydrolysis rates, and slight underestimation of molecular masses on the order of 5% may thus be expected.

The Light Scattering Kinetic Assay Method. For simultaneous multiangle measurements of the light scattered from the HA solutions undergoing hydrolysis, special software was written for a Wyatt Technology Dawn F light scattering unit operating in the batch mode. The inventor of the instrument and his co-workers have given several accounts of its capabilities.[10,11] The unit employs a vertically polarized He–Ne laser at 632 nm and simultaneously samples the relative scattering intensity from 15 sequential scattering angles chosen from a group of 18 ranging, for aqueous solutions, from about $\theta = 9°$ to 170°.

A normalization and calibration data file was created prior to the series of depolymerization experiments by measuring and storing, at each of the 15 angles, the photodiode dark counts, the scattering from pure solvent, the scattering from a reference solvent, toluene in this case, for which the absolute Rayleigh ratio is 1.407×10^{-5} cm^{-1}, at 25 °C at $\lambda = 632$ nm, and the scattering from a strong isotropic scatterer (10 mg/mL cetyltrimethylammonium bromide (CTABr) micelles in aqueous 10 mM KBr, in this case) for normalization.

For samples undergoing depolymerization the relative scattering at each angle at a chosen sampling interval time was measured and the normalization/calibration data used in storing the angular Kc/I data to the microcomputer's hard disk. Because the hydrolysis was so slow, sample times were never separated by less than 10 s. Since the A/D board used for reading the diode voltages has a sampling speed of 27.5 kHz in the direct memory access mode (DMA), sampling times could in principle be reduced to milliseconds, depending on the intervening calculations and computer I/O functions, should the need arise in much more quickly depolymerizing systems. Index of refraction effects for interfacial scattering and variation in scattering volume between water and toluene were taken to roughly cancel in the absolute calibration.

Alternatively, single angle light scattering measurements were made on a separate, thermostatable system using an argon ion laser operating at 488 nm. This system was also used for the dynamic light scattering studies of hydrodynamic radii. Details have been given elsewhere.[6] The value of 3.96×10^{-5} cm^{-1} was used for the absolute Rayleigh ratio for toluene at 25 °C at λ = 488 nm.

The value of $dn/dc = 0.176$ was taken from ref 12, and used for HA in both the aqueous NaOH solutions and those containing DMSO (dimethyl sulfoxide). It should be noted that widely varying values of dn/dc have been reported for HA (a partial summary appears in ref 6) and there is still room for a definitive determination.

HPLC and Static Light Scattering Detection. An ISCO Model 2350 isocratic pump was used in conjunction with an ANSPEC ERC-7522 refractive index detector, r.i. An Alltech AQ GPC GB 100,000 Å (catalog no. 100777), resin based column (250 mm long × 10 mm diameter), provided fair separation characteristics for HA when an eluant of 0.1 M aqueous NaOH/DMSO in 80/20 volume ratio was used. Purely aqueous eluants with added salt with no adjustment to high pH values led to retention of HA in the column. Even in the NaOH/DMSO solvent polystyrenesulfonate (NaPSS) standards showed highly retarded passage from the column and eluted after the salt peak. Such calibration standards were hence useless for MW determination.

The HPLC flow passed through a precolumn filter with a 0.5-μm frit and 0.02 in. diameter through hole into the flow cell of the Wyatt Dawn-F scattering photometer and then into the r.i. cell. Fifteen scattering angles and the r.i. detector output were collected and stored simultaneously, typically at 1-s intervals, with the pump rate at 1.5 mL/min. A 250-μL injection loop was used, and HA samples were generally injected at a concentration of between 0.25 and 1.0 mg/mL.

The "dead volume" between the active part of the r.i. detector and the Dawn flow cell was estimated, geometrically and by peak measurements with the HPLC column removed, to be about 0.30 mL. Even small uncertainties in dead volume can have large effects on the analysis of GPC results.[13]

Software was written to analyze the combined r.i. and scattering data. The absolute angular Rayleigh ratio $I(q)$ and concentration c was determined at each point and the molecular weight M and the mean square radius of gyration were then calculated at each point according to the standard equation

$$\frac{Kc}{I(q)} = \frac{1}{M}(1 + q^2\langle S^2\rangle/3) + 2A_2c \qquad (10)$$

Because the HPLC column separates the HA into narrow mass increments sampled at each point in time by the detectors $M_z \simeq M_w \simeq M_n$ and $\langle S^2\rangle_z \simeq \langle S^2\rangle_w \simeq \langle S^2\rangle_z$. Diffusion broadening effects are ignored.

Using the in-line filter led to pleasingly clean light scattering data, with virtually no wild swings at any angle due to "dust" or other anomalous scatterers. No data smoothing was hence needed, although occasional isolated bad points were routinely removed from spectra.

Results

Results on Unhydrolyzed HA. In order to analyze the base hydrolysis rates and fragment distribution of HA, the unhydrolyzed material was characterized. There have been many attempts to measure different physical properties of HA with light scattering,[6,12,14] viscosity,[4] transient electric birefringence,[15] etc. A summary of some of this work is given in ref 6.

Particularly relevant to the current experiments are the results on how $\langle S^2\rangle$ and A_2 vary as a function of ionic strength Cs. $\langle S^2\rangle$ (in Å^2) was approximated in ref 12 as

$$\langle S^2\rangle = \frac{Mb}{3\,m}[87 + 307C_s^{-0.5}] \qquad (11)$$

where Cs is in mM and b/m is the contour length per unit mass of HA, taken as about 40 Å/Da. The results were obtained on the same HA as in this work, for which M_w is around $(1.35 \times 10^6) \pm (0.25 \times 10^6)$. The linear dependence of $\langle S^2\rangle$ on M in eq 11 was *assumed* in ref 12. An experimentally based estimate of the true scaling law is given below.

A_2 (mL mol/g^2) can be taken from Figure 3 in ref 12 to vary with C_s (in mM) as roughly

$$A_2 = 0.03C_s^{-0.5} \qquad (12)$$

Preliminary light scattering experiments on HA in NaOH solutions quickly reconfirmed earlier reported conclusions[4,6] that the HA random coil undergoes a contraction at high NaOH. We experimentally quantified this result here by using the single concentration technique of ref 12 (approximation for high angles) for estimation of $\langle S^2\rangle$ and A_2 vs [NaOH] for solutions originally at 0.25 mg/mL [HA] and 150 mM NaCl. $M_w = 1.35 \times 10^6$ was used in the single concentration method. Parts a and b of Figure 1 show the variation of R_g and A_2 vs [NaOH], respectively. Experiments were performed within minutes of injecting the desired NaOH to ensure that only negligible hydrolysis occurred. The results in Figure 1a,b are thus referred to as "zero time" results.

Error limits on the absolute values of $\langle S^2\rangle^{0.5}$ and A_2, due to uncertainties in dn/dc, concentrations, and other systematic errors are roughly ±12% and ±25%, respectively. Uncertainties due to random errors such as noise in the scattering data and fitting errors are typically less than 3%.

Also shown on Figure 1a,b are the results obtained when NaCl is added to the original solution (already at 150 mM NaCl) instead of NaOH. It is clear that the large decreases in both A_2 and R_g with increasing NaOH are not merely ionic strength effects. In fact, the "apparent intrinsic persistence length" L_0' (amply defined and discussed in refs 12, 16, and 17) obtained from extrapolation of the total apparent persistent length L_T' to infinite NaCl (on a plot of L_T' vs $1/C_s^{0.5}$, for which the highest linearity obtained[12,16]) is about 87 Å. Taking the plateau region at high NaOH in Figure 1a gives an $L_T' = 40$ Å. Thus, the HA undergoes a large loss of intrinsic stiffness at high NaOH. The high NaCl and NaOH values of A_2 are, respectively, about 1.5×10^{-3} and 0.5×10^{-3}.

Remarkably different are the results concerning hydrodynamic radius D_h vs [NaOH]. These values, which have been corrected for the slight increase of viscosity as [NaOH] increases (the formula $\eta = 0.089 + 2.136$[NaOH] (in mM) at T = 25 °C was fit from the data in the *CRC Handbook of Chemistry and Physics*), are shown in Figure 1c. They were obtained from $\theta = 90°$ measurements on a 0.25 mg/mL solution of HA originally at 150 mM NaCl, to which aliquots of NaOH were added. This concentration is low enough to ensure that the value of D_h thus obtained is within error bars (about 3%) of the extrapolation of Dh to zero HA concentration.[12] The very slight drop in D_h at high NaOH may be from early effects of NaOH hydrolysis on the serially titrated sample. This independence of D_h from R_g, which changes strongly with [NaOH] (Figure 1a) seems to be another manifestation of some type of peculiar partial draining behavior, which has now been observed for several linear polyelectrolytes.[12,16,18] In fact, for HA, R_g increased by a factor of 70% from [NaCl] = 2 to 300 mM, whereas D_h, as obtained by extrapolations to zero HA concentration, remained constant.[12]

Unfortunately, the undigested HA passed mostly through the exclusion volume of the column, so that initial polydispersity information is not available. Since the limiting high u_0 case is used for determining β and $\hat{r}$ (eqs 4 and 2), however, this is not overly troubling.

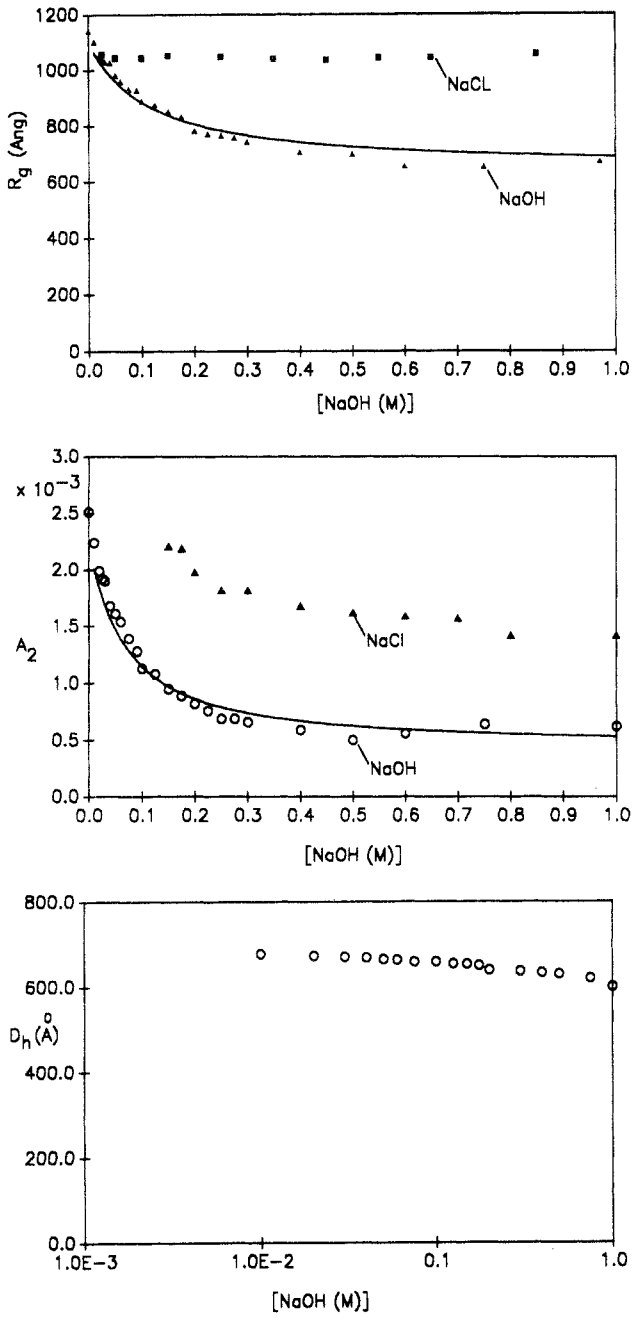

Figure 1. (a, top) $\langle R_g \rangle$ vs [NaOH] (▲), original solution at 0.25 mg/ml [HA] and 150 mM [NaCl] for time = 0. Values are appropriate to HA polymers of $M_w = 1.35 \times 10^6$. Solid line is the prediction, with no adjustable parameters, according to the destiffening model in the discussion, by eqs 20 and 24. ■ is for [NaCl] over and above the original 150 mM NaCl solution, when NaCl was added instead of NaOH. (b, middle) A_2 vs [NaOH] (○) for the same solution as in Figure 1a. The solid line is the prediction according to eq 25. ▲ is for NaCl added to original solution instead of NaOH. (c, bottom) Hydrodynamic radius, D_h, vs [NaOH] for the same solution conditions as in parts a and b. There is no measurable change in D_h, even though $\langle S^2 \rangle^{0.5}$ varies significantly.

Hydrolysis Rates. Figure 2 shows the time course of Kc/I at $\theta = 90°$ and $T = 25$ °C from the Wyatt instrument for the alkaline hydrolysis of HA at a variety of [NaOH]. [HA] = 0.5 mg/mL for all the experiments represented. The steeper slopes of Kc/I vs t for higher [NaOH] reflect the higher rate of hydrolysis, whereas the lower intercepts show the effect of decreasing A_2 with increasing [NaOH], as already seen for the $t = 0$ data of Figure 1b.

Figure 3 shows the hydrolysis rates $\dot{r}$ plotted vs [NaOH] as obtained from Kc/I data, such as in Figure 2. $\dot{r}$ is calculated by eqs. 4 and 2 using an original mass of 10^6 for

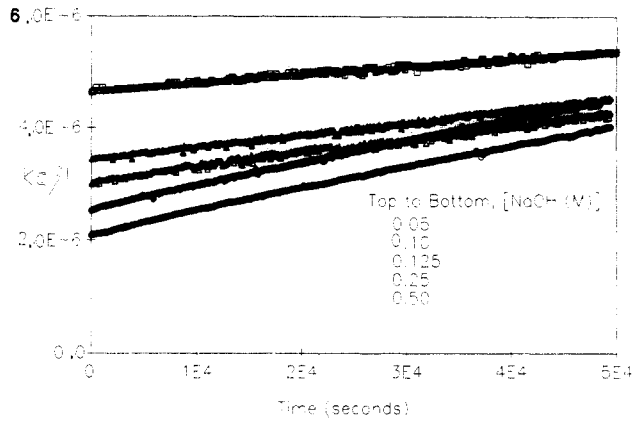

Figure 2. K_c/I vs time for base hydrolysis of HA at $T = 25°$ using the Wyatt system. Different [NaOH] curves are shown.

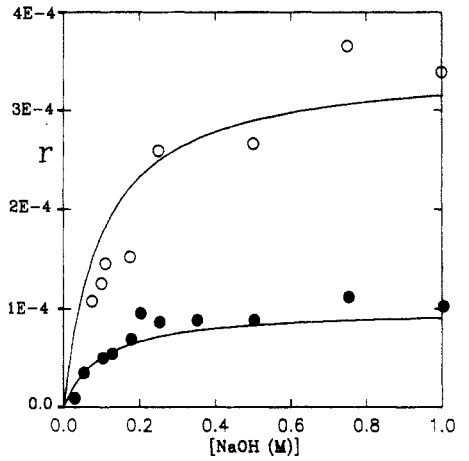

Figure 3. Base hydrolysis rate constants (average bonds broken per megadalton of original polymer per time) vs [NaOH]. Upper points are for $T = 36$ °C (argon ion laser system); lower points are for $T = 25$ °C (Wyatt system). Solid lines are according to eq 13 with pK = 13.0.

convenience, so that $\dot{r}$ represents the average number of bonds broken per second per 1 MDa polymer. $\dot{\beta}$ is simply $\dot{r} \times 10^{-6}$. A conservative systematic error estimate on $\dot{r}$ is around ∓20%.

Interestingly, the rates are not linear vs [NaOH], implying that the bond hydrolysis is not a simple first-order reaction in [NaOH]. Rather, the shape of the data suggests a titration-dependent phenomenon, involving the HA itself. In fact, if the data are fit with a function of the form

$$\dot{r} \propto \frac{10^{(\mathrm{pH}-\mathrm{p}K)}}{1 + 10^{(\mathrm{pH}-\mathrm{p}K)}} \qquad (13)$$

where the proportionality constant is set to the experimental plateau value and the pK is taken as the only adjustable parameter, the solid lines in Figure 3 are obtained for pK = 13.0. This most likely corresponds to the pK of the –OH group on the glucosamine rings, ionization of which might lead to a nucleophilic attack by the residual $-O^-$ on the neighboring glycosidic bond, resulting in the depolymerization of the HA molecule. Thus, in this scenario, the base hydrolysis of HA is due to an intramolecular bond cleavage mechanism, the rate of which is controlled by the pH of the supporting medium.

Because the hydrolysis reaction seems to be intramolecular in nature, the rate constant $\dot{r}$ should be independent of [HA]. In fact, $\dot{r}$ was found to be independent of [HA] over the range 0.25–1.0 mg/mL. We point out that [HA] at 0.5 mg/mL gives roughly 1.25 mM of scissile glycosidic

bonds [B] at the outset of hydrolysis, so that [NaOH] ≫ [B] for all [NaOH] used.

Time Course of $\langle S^2 \rangle$, M_w, and Fragment Distributions from Hydrolysis. (i) Batch Scattering Results. For polydisperse ideal coils for which $q^2\langle S^2 \rangle > 3$, the scattering behavior is approximated by[3]

$$\frac{Kc}{I(q)} = \frac{1}{2M_n} + \gamma q^2/2 + 2A_2c \tag{14}$$

where γ is the proportionality factor in $\langle S^2 \rangle = \gamma M$, applicable over all M where the polymer resembles an ideal coil. The slope of Kc/I, $P \equiv d(Kc/I)/dq^2$, at *high* angles should thus be roughly constant as the depolymerization proceeds. In fact if a scaling law of the type

$$\langle S^2 \rangle = aM^{\upsilon} \tag{15}$$

exists, and $2A_2c$ is independent of angle, it then follows from eq. 10

$$\frac{d(Kc/I(q))}{dq^2} = \frac{a}{3}M^{\upsilon-1} \tag{16}$$

This is an interesting property of $d(Kc/I)/dq^2$ and shows that P remains constant as M changes for ideal coils (υ = 1). Although eq 14 is not expected to hold for excluded volume coils, it is only in the limit of high u that $Kc/I(q)$ should vary as $q^{2/\upsilon}$. Recent experimental data and Monte Carlo simulations indicate, however, that in the approximate range of $3 < u < 50$ $Kc/I(q)$ still varies roughly as q^2. Hence, if excluded volume effects are present ($\upsilon \simeq 1.2$), P should decrease as depolymerization proceeds for large u.

On the other hand, in the low u (low angle) limit

$$P = \frac{\langle S^2 \rangle_z}{3M_w} \tag{17}$$

For ideal coils P should increase as M_z/M_w as depolymerization proceeds and polydispersity increases, where M_z and M_w are given by eqs 8 and 9. P should increase at a somewhat higher rate for excluded volume coils.

Figure 4a shows $P^{-1}(u) = (Kc/I - 2A_2c)$ normalized to 1 at $t = 0$ for a typical 0.5 mg/mL HA solution undergoing hydrolysis at $T = 25$ °C in 0.75 M NaOH. The experimental rate constant of $\dot{r} = 0.93 \times 10^{-4}$ was used to determine the value of r, for which the lines are drawn according to eq 1.

As concerns the slopes in Figure 4a, the theoretical lines have constant slope as predicted by eq 1, P at high angles decreases slightly with r, most likely reflecting excluded volume effects, and P at low angles increases. Figure 4b shows the time course of the low and high angle slopes.

Using the values of A_2 from Figure 1b and the low angle extrapolation of the time-dependent scattered intensity to zero angle $I(t,0)$, M_w vs t for the hydrolysis experiments was calculated by eq 10. A typical result of this is shown in Figure 4c, for the case where [NaOH] = 1.0 M and [HA] = 0.5 mg/mL. Shown on the same figure is $\langle S^2 \rangle_z^{1/2}$ vs t.

(ii) HPLC Results on Hydrolysis Fragments. Figure 5a shows $c(M)$ vs M for HPLC/light scattering data from HA at different stages of NaOH hydrolysis. The solutions were at 0.5 mg/mL HA, with 150 mM NaCl, and contained 1 M NaOH. The hydrolyses were carried out at $T = 25$ °C. The distributions clearly show the progressive degradation of the HA by NaOH. The dotted lines show the corresponding predicted distributions according to eq 6b, assuming an originally monodisperse population. The

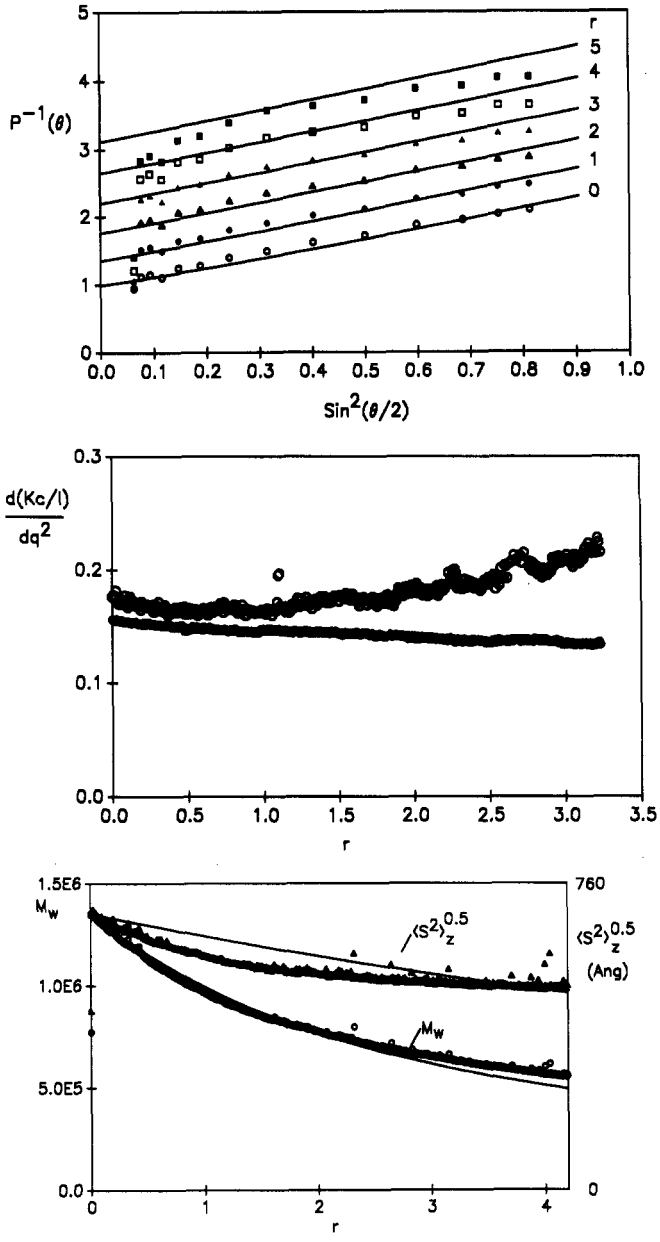

Figure 4. (a, top) Inverse scattering form factor $P^{-1}(u)$ vs $\sin^2(\theta/2)$, at different points in the digestion, for $r = 0$ to 5. [HA] = 0.5 mg/mL, [NaOH] = 0.75 M, and $T = 25$ °C. The solid lines are the predictions according to eq 1 for ideal coils. (b, middle) $P \equiv d(Kc/I)/dq^2$ vs r for high angles (lower curve, $\theta = 59$–$129°$) and low angles (upper curve, $\theta = 26$–$45°$). The increase for the low angle slope is due to the increasing polydispersity (eq 17), whereas the decrease for the high angle slope is most likely due to excluded volume effects; $\upsilon > 1$ in eq 16. (c, bottom) M_w vs r. Solid lines show the theoretical prediction for M_w using $\dot{r} = 0.93 \times 10^{-4}$. Also shown is $\langle S^2 \rangle_z$ vs r for the same data. Solid line is from M_z in eq 9 scaled to R_g, and assumes $\upsilon = 1.0$ in eq 15.

agreement is qualitatively good, although the predicted distributions have longer trailing edges at low M than the actual data show.

Figure 5b shows $M_w/M_{w,0}$ and $M_z/M_{z,0}$ vs r, as given by eqs 8 and 9. $\dot{r}$ is taken as 0.93×10^{-4} bonds per second per original megadalton polymer of HA. The experimental points come from the $c(M)$ distributions in Figure 5a. The agreement between the experimental and theoretical points is quite good. The inset to Figure 5b shows the predicted time course of M_w/M_n and M_z/M_w from eqs 7–9, together with these values calculated from the experimental $c(M)$ curves in Figure 5a. Again, the agreement is good. As an illustration of the effect of dead volume, the triangles in the inset are the values of M_z/M_w which

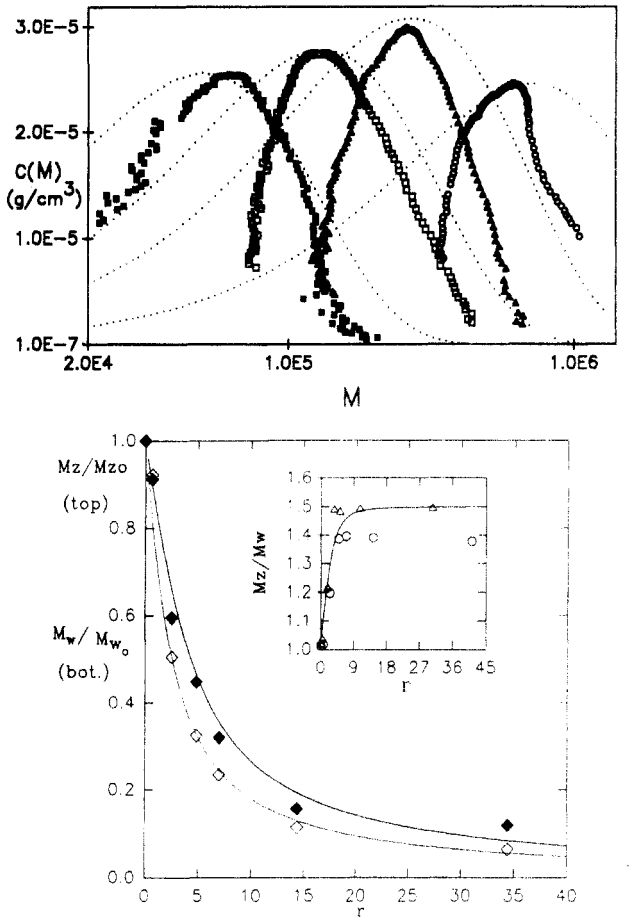

Figure 5. (a, top) HPLC chromatograms of fragments from HA hydrolyzates under conditions [NaOH] = 1 M, [HA] = 0.5 mg/mL, T = 25 °C, at: ○, 7 h (r = 2.52); △, 21 h (r = 7.5); □, 45 h (r = 16.2); ■, 120 h (r = 43.2). Dotted lines show calculated distributions according to eqs 6a,b. (b, bottom) $M_w/M_{w,0}$ ($M_{w,0}$ is the initial M_w) (◇) and $M_z/M_{z,0}$ ($M_{w,0}$ is the initial M_w, likewise for $M_{z,0}$) (◇) vs r, using experimental distributions from Figure 5a. Lines are calculations according to eqs 8 and 9. Inset is the polydispersity ratio M_z/M_w according to eqs 8 and 9: ○, 0.3 mL dead volume; △, 0.25 mL dead volume.

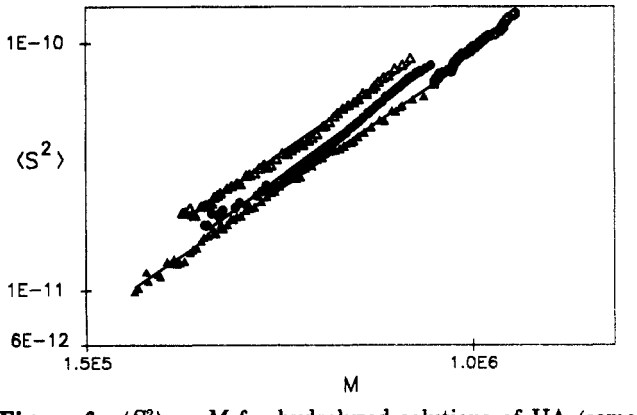

Figure 6. $\langle S^2 \rangle$ vs M for hydrolyzed solutions of HA (same conditions as Figure 5a): ○, 2 h; ●, 7 h; △, 14 h; ▲, 21 h. The slope is ν = 1.30 for a dead volume of 0.3 mL, and ν = 1.12 for 0.25-mL dead volume.

result when a dead volume of 0.25 mL is used instead of 0.30 mL (which has been used throughout).

Figure 6 shows log $\langle S^2 \rangle$ vs log(M) for several of the curves from Figure 5a. Although there is some spread in the absolute values of $\langle S^2 \rangle$, the exponent is fairly consistent and gives ν = 1.30. This is not far from what is normally expected for random coils with excluded volume.[23] This slope is found to be quite sensitive to changes in the

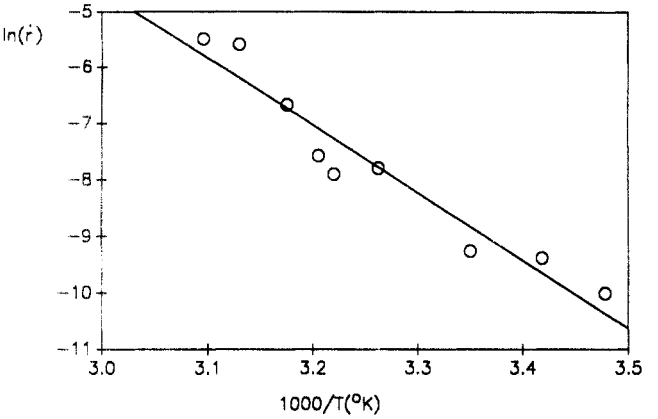

Figure 7. Rate constant $\dot{r}$ vs 1000/T (K) for [NaOH] = 1 M, from the argon ion system, for determination of activation energy.

estimate of dead volume and other errors, however, and is hence not presented as a strong confirmation of the theoretical excluded volume predictions. Using 0.25 mL dead volume instead of 0.30, for example, gave ν = 1.16. Such experimental data, in order to have any hope of distinguishing between a slope of 1.0 (ideal coil) and 1.20 (coil with excluded volume), require a rigorous error analysis of dead volume and other effects.[13]

Estimation of Activation Energy for the Base Hydrolysis of HA. In order to estimate the activation energy U_{ac} for the base hydrolysis reaction, the hydrolysis rate constant $\dot{r}$ was determined by the time-dependent light scattering assay at a variety of temperatures from 14 to 50 °C using the argon ion system fixed at θ = 90°. HA solutions (0.5 mg/mL) were hydrolyzed with 1 M NaOH in these experiments. A simple exponential dependence for $\dot{r}$ was assumed

$$\dot{r} = A \exp(-U_{ac}/k_B T) \qquad (18)$$

A plot of ln($\dot{r}$) vs $1/k_BT$ is shown in Figure 7, from which an activation energy of about 1.03 eV, or 23.4 kcal/mol, can be estimated. This can be compared to the activation energy of 30.5 kcal/mol found for the acid hydrolysis of HA in 6 M HCl.[19]

Discussion

One of the most salient features of HA behavior at high pH is that titration of the hydroxyl groups to yield –O⁻ appears to control two distinctly different phenomena with vastly different activation barriers and rate constants: a very rapid loss of hydrogen bonds leading to loss of helical secondary structure and large destiffening of the HA coil, and the slow, intramolecular cleavage, or hydrolysis, of glycosidic bonds.

To emphasize how these distinct phenomena are controlled by the same titration behavior, Figure 8 shows the hydrolysis rate constants, and the negative, arbitrarily scaled values of R_g and A_2 vs [NaOH]. The behavior of the three quantities shares the same dependence of [NaOH], and all three quantities give a pK value of around 13.

Simple Model for the Destiffening of the HA Coil with Increasing [NaOH]. We propose here a simple model for the destiffening of the HA coil as [NaOH] increases, based on the hypothesis that titration of the –OH group to –O⁻ leads to the destruction of local hydrogen bonds, with a corresponding shortening of the apparent intrinsic persistence length, L_0'. References 12, 16, and 17 give a full account of the meaning of the term "apparent" in the persistence length definition and of its use within the wormlike chain model. Formulations of the electro-

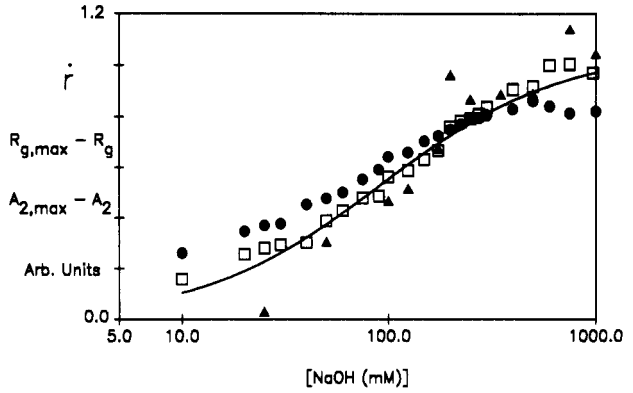

Figure 8. Superposition of conformational, interaction and hydrolysis parameters to show their titration-controlled nature: ▲, hydrolysis rates $\dot{r}$ from Figure 3; □, $-R_g([NaOH]) + R_g([NaOH] = 0)$ from Figure 1a, arbitrarily scaled; ●, $-A_2([NaOH]) + A_2([NaOH] = 0)$, from Figure 1b, arbitrarily scaled.

static persistence length model and electrostatic excluded volume effects are treated in refs 20–26.

The "apparent" intrinsic, electrostatic, and total persistence lengths are denoted as primed quantities, respectively as, L_0', L_e', and L_T, where $L_T' = L_0' + L_e'$. The apparent persistence length effectively lumps together both the local stiffening and long range excluded volume effects and, as such, may be found to be an objectionable quantity by some theorists. The value of the apparent persistence length concept resides, however, in its surprisingly consistent experimental behavior,[12,16,18,27] which has also manifested the same behavior under Monte Carlo simulations.[17] Namely, it has been found that

$$L_T' \propto \xi/C_s^{0.5} \tag{19}$$

where ξ is the polyelectrolyte's linear charge density, and C_s is the ionic strength of the medium. This relation has been found for $C_s \sim 1$ mM to 4 M. It may fail for lower C_s. This L_T' works well when substituted into the standard wormlike chain formula as

$$\langle S^2\rangle = LL_{T/3}' - L_T'^2 + 2L_T'^3/L - 2(L_T'^4/L^2) \times [1 - \exp(-L/L_T)] \tag{20}$$

in place of L_T, and the actual measured, perturbed $\langle S^2\rangle$ is used in place of the unperturbed $\langle S^2\rangle_0$. It is still a challenge for theorists to understand the origin of this result.

According to ref 12, HA in univalent and divalent salts[28] is characterized by an apparent total persistence length of

$$L_T'(\text{Å}) = 87 + 305/C_s^{0.5} \tag{21}$$

where 87 Å is L_0'.

We now define the model for the destiffening of HA. Consider HA to be a single stranded molecule with short lengths of hydrogen bond stabilized helical structure which gives it an intermediate intrinsic stiffness between very stiff molecules like DNA[29] (600 Å) and xanthan (310 Å)[30] and very flexible polymers like sodium polystyrenesulfonate[18] ($L_0' \sim 30$ Å) and sodium polyacrylate[16] ($L_0' =$ 27 Å). The linear shape of $Kc/I(q,t)$ vs t is evidence for lack of double stranding for HA or higher associations in the conditions studied. Since these short helical segments may be fairly random L_0' most likely represents an average persistence length, rather than being related to a single, well-defined bending energy. Suppose that when all hydrogen bonds are broken (at high [NaOH]), the final dimensions of the HA coil reflect its residual or contracted apparent intrinsic persistence length $L_{0,c}'$, which is due to factors such as intermonomer bond angle, rotameric states, and steric exclusion.

Figure 1a shows that $\langle S^2\rangle^{0.5}$ is around 670 Å for 1.35 MDa HA at high [NaOH]. From eq 20 this gives $L_{0,c}' =$ 40 Å; i.e. the contracted apparent intrinsic persistence length is less than half that when the hydrogen bonds are intact. The high angle value of $P(r = 0)$ from 4b gives a similar value using $L_T' = 6mP/l$, where $l/m = 40$ Å/Da is the approximate mass per unit contour length of HA.

As the hydrogen bonds "pop" with increasing [NaOH] the average apparent intrinsic persistence length should change. Let $W(L_T',C_s,[NaOH])\,dL_T'$ represent the normalized fraction of monomer links with L_T' between L_T' and $L_T' + dL_T'$ at a given [NaOH] and C_s. Then

$$L_T'(C_s,[NaOH]) = \int L_T' W(L_T',C_s,[NaOH]\,dL_T' \tag{22}$$

A model for $W(L_T,C_s,[NaOH])$ is now needed. The simplest assumption is to ignore any complex effects of cooperativity among the H bonds on $W(L_T,C_s,[NaOH])$ and simply consider a bimodal distribution; i.e. all groups with –OH intact will have L_T' given by eq 21 above, denoted by $L_T'(C_s)$ and all titrated groups $-O^-$ will have $L_T' = L_{0,c}' =$ 40 Å. This assumption may not be bad, considering that L_T' given by eq 21, is already an average over segments of varying local stiffness and successfully predicts HA dimensions over a wide range of C_s. Then

$$W(L_T',C_s,[NaOH]) = \frac{1}{[1 + 10^{(pH-pK)}]} \times (\delta(L_T' - L_T'(C_s)) + \delta(L_T' - L_{o,c}')10^{(pH-pK)}) \tag{23}$$

With this and pH = log[NaOH]

$$L_T'(C_s,[NaOH]) = \{L_T'(C_s) + L_{0,c}'10^{(pH-pK)}\}/[1 + 10^{(pH-pK)}] \tag{24}$$

whence $\langle S^2\rangle$ can be computed via eq 20. The solid line in Figure 1a is $\langle S^2\rangle^{0.5}$ calculated by eq 20, using L_T' from eq 24, with $pK = 13.0$, which was computed from the best fit to the rate constants in eq 13. The prediction falls virtually on top of the data and can be considered to be a quantitative match. Importantly, after the pK_a is determined from eq 13, there are no adjustable parameters in this model. C_s is taken to be [NaCl] + [NaOH].

The behavior of A_2 vs [NaOH] is somewhat more complicated, and a very simple argument is used here instead of an in-depth analysis based on existing expressions for A_2 or wormlike chains. A_2 basically measures excluded volume per mass squared of the polymer. The volume of the coil can be thought to go as about $\langle S^2\rangle^{1.5}$. Then, in the coil limit and at high C_s where the electrostatic portion of the total excluded volume is small, A_2 should scale as

$$A_2([NaOH]) = A_2(C_s{=}150\text{mM}) \times [L_T'(C_s = 150\text{mM})/L_T'(C_s,[NaOH])]^{1.5} \tag{25}$$

where L_T' (C_s=150mM) is from eq 20 and $L_T'(C_s,[NaOH])$ is from eq 24. The solid line in Figure 1b shows the result of eq 25. It is a good quantitative match to the data. In Figure 1b the values of A_2 were computed with $M = 1.35 \times 10^6$ in eq 20, which gives a match to the full Zimm plot value of about 4.5×10^{-4} at high [NaOH].

We point out that the term "contraction" of the HA coil has been used here instead of "collapse", since the state of HA as NaOH increases should still resemble a random coil, not a globule.

The Constancy of D_0 vs [NaOH]. The constancy of D_0 vs [NaOH] seen in Figure 1c, in the face of the strongly varying R_g vs [NaOH] in Figure 1a, is a continuation of the puzzle reported in other recent works, in which D_0 vs C_s remained constant, whereas R_g varied strongly with C_s.[12,16,18] While the possible influence of internal modes on the autocorrelation function has been previously eliminated as the origin of the effect,[12,16] the most obvious conjecture, namely simple free-draining of the polymer coil, also does not seem likely.[18]

The notion that $D_0 \propto M^{-0.5}$ for polymers and polyelectrolytes, i.e. that they behave hydrodynamically in the nondraining limit, is taken as a virtual article of faith in such "sizing" techniques as dynamic light scattering. The gradual accumulation of data on various linear polyelectrolytes showing that D_0 does not necessarily measure size means that such techniques must be approached with caution.

Until a firm theory for this behavior is found, further experimental details are desirable. It does seem that the independence of D_0 from R_g is related to some type of draining effect (intermediate level of hydrodynamic perturbation among resistive elements in the polymer chain) but not to a naive fully free-draining limit. There is evidence that the bulk or hydrated volume of the polyelectrolyte sidegroups has a large influence on the relation between D_0 and R_g.[12,16,18,27,31]

It might be thought that the stiffness of the polyelectrolyte may also influence the degree of draining, stiffer coils being more likely to have less hydrodynamic perturbation among units and more draining. NaPAA is quite flexible, however, with an apparent intrinsic persistence length L_0' of around 27 Å, and yet gives D_0 independent of R_g. In the present case HA, which destiffens from L_0' = 87 Å to L_0' = 40 Å, continues to give D_0 independent of R_g, so that the essential "baldness" of the HA continues to control this phenomenon.

It should be pointed out that, although the contraction of R_g for HA is consistent with ref 6, D_0 was found to increase at high pH in the latter work. As has been pointed out since,[3,12] the HA used in that work had a slight protein contamination which rendered it an ill-behaved polyelectrolyte, at least from the point of view of light scattering (e.g. the scattering intensity was independent of C_s, in stark contrast to the usual enormous increase in intensity as C_s increases for polyelectrolytes). The bacterial HA used in this and other works[3,12] has been shown to be of very high purity, manifests classical polyelectrolyte properties, and is free of any "extraordinary phase" of diffusion, recently traced to residual populations of aggregates and/or other particulates.[32]

Evaluation of Hydrolysis Fragment Distributions and Scaling Laws. Figure 2 shows that the degradation of HA by NaOH resembles a random scission process and cannot be, for example, an endwise cleavage process, as the prediction for the light scattering behavior would be quite different.[1,3] Additionally, HA in the NaOH solutions cannot exist as associated double or multiple strands, as Kc/I would curve upward in time, rather than increase linearly.

Figure 4 shows that the fragment distributions, eqs 6a,b, which were used to compute the mass averages in eqs 7–9, make fairly good predictions for the experimentally determined time course of M_w and z-average R_g. These latter quantities were determined wholly in the batch mode, and were possible to obtain due to the simultaneous monitoring of scattering at many angles by the Wyatt instrument.

Due to the large effects that dead volume and other effects have on the interpretation of the HPLC/light scattering results, Figures 5a,b and 6 are only preliminary at this point. Qualitatively, Figure 5a clearly shows the progressive degradation and broadening of the HA population, with good qualitative agreement with the theory, especially as far as the progress of the peak locations with increasing hydrolysis time. The course of M_z, M_w, and M_z/M_w as calculated from these distributions is in fairly good accord with the theory.

Intramolecular Hydrolysis. We do not attempt to analyze the actual chemical processes involved in the degradation of the HA. The titration-curve nature of the rate constants, however, disallows a direct bimolecular reaction between the scissile HA bonds and bulk OH^-. Mechanisms for intramolecular hydrolysis (anchiomeric assistance) of different types of sugars have been proposed by various groups of chemists.[33–36] The independence of the rate constant $\dot{r}$ from [HA] over the range 0.25 to 1.0 mg/mL suggests that for a given scissile bond, the $-O^-$ groups from separate HA chains do not participate significantly in the hydrolysis.

The titration-curve type behavior of the hydrolysis has an interesting implication for HA chemical processes at high [NaOH]. Namely, if one is seeking to maximize the rate of a genuine bimolecular reaction between HA and another species at high [NaOH] and to minimize the amount of hydrolysis, it may actually be advantageous to run the reaction at the highest possible [NaOH], out on the hydrolysis rate plateau, for a short time rather than at low [NaOH] for a longer time. This will be true, for example, if the bulk OH^- participates in a bimolecular reaction with HA, and for any reagent who's reaction rate increases with [NaOH] while the hydrolysis rate is essentially on the plateau.

Conclusions

Titration of –OH groups on HA by NaOH to yield $-O^-$ leads to (i) the virtually instantaneous destruction of hydrogen bonds with subsequent destiffening of the HA random coil into a much more compact, flexible random coil with correspondingly reduced A_2 and (ii) the very slow hydrolysis of the HA polymer in what appears to be an intramolecular scission process. These processes, as measured by R_g, A_2, and the hydrolysis rate constants, show mutually overlapping titration-curve-like behavior, from which a pK of about 13.0 for the –OH groups can be estimated (Figure 8).

Complementary experiments, sensitive to H-bond structures (NMR, Raman, etc.) would be valuable in determining whether H-bonds are really broken in NaOH as proposed.

Although polysaccharides vary enormously in chemical make-up, stereochemistry, etc., the –OH group is nonetheless a universal motif among them, so that NaOH-induced conformational changes and similar hydrolyses mechanisms may be quite common. Especially interesting might be the study of polysaccharides for which evidence of double or triple helix structure in solution has been found.[37,38] It is hoped that the type of combined light scattering techniques presented here will prove to be a powerful, efficient and general way of characterizing polysaccharide behavior at high pH.

Acknowledgment. Support from NSF Grants NSF MCB9116605 and NSF INT-9101058 are gratefully acknowledged. We thank Larry Byers for many helpful

conversations and for the suggestion that HA cleavage could be an intramolecular phenomenon.

References and Notes

(1) Reed, C. E.; Reed, W. F. *J. Chem. Phys.* **1989**, *91*, 7193.
(2) Reed, C. E.; Reed, W. F. *J. Chem. Phys.* **1990**, *93*, 9069.
(3) Reed, W. F.; Reed, C. E.; Byers, L. D. *Biopolymers* **1990**, *30*, 1073.
(4) Morris, E. R.; Rees, D. A.; Welsh, E. J. *J. Mol. Biol.* **1980**, *138*, 383.
(5) Scott, J. E.; Hentley, F.; Moorcroft, D.; Olavesen, H. *Biochem. J.* **1981**, *199*, 829.
(6) Reed, C. E.; Li, X.; Reed, W. F. *Biopolymers* **1989**, *28*, 1981.
(7) Reed, C. E.; Reed, W. F. *J. Chem. Phys.* **1992**, *97*, 7766.
(8) Lowry, O. H.; Rosebrough, N. J.; Farr, A. L.; Randall, R. J. *J. Biol. Chem.* **1951**, *193*, 265.
(9) Farndale, R. W.; Sayers, C. A.; Barret, A. J. *Connect. Tissue Res.* **1982**, *9*, 247.
(10) Wyatt, P. J.; Jackson, C.; Wyatt, G. K. *Am. Lab.* **1989**, *20* (5), 86.
(11) Jackson, C.; Nilsson, L. M.; Wyatt, P. J. *J. Appl. Polym. Sci., Appl. Polym. Symp.* **1989**, *43*, 99.
(12) Ghosh, S.; Li, X.; Reed, C. E.; Reed, W. F. *Biopolymers* **1990**, *30*, 1101.
(13) Reed, W. Manuscript in preparation.
(14) Cleland, R. *Biopolymers* **1968**, *6*, 1519.
(15) Trimm, H. H.; Jennings, B. R. *Biochem. J.* **1983**, *213*, 671.
(16) Reed, W. F.; Ghosh, S.; Medjhadi, G.; François, J. *Macromolecules* **1991**, *24*, 6189.
(17) Reed, C. E.; Reed, W. F. *J. Chem. Phys.* **1991**, *94*, 8479.
(18) Peitzsch, R. M.; Burt, M.; Reed, W. F. *Macromolecules* **1992**, *25*, 806.
(19) Cleland, R. L. *Arch. Biochem. Biophys.* **1977**, *180*, 57.
(20) Landau, L. D.; Lifshitz, E. M. In *Statistical Physics*, 3rd ed.; Pergamon Press, Inc.: Oxford, 1980; Part 1.
(21) Odijk, T. *J. Polym. Sci., Polym. Phys. Ed.* **1977**, *15*, 477.
(22) Skolnick, J.; Fixman, M. *Macromolecules* **1977**, *10*, 944.
(23) Yamakawa, H. *Modern Theory of Polymer Solutions*; Harper and Row: New York, 1971.
(24) Odijk, T.; Houwaart, A. C. *J. Polym. Sci., Polym. Phys. Ed.* **1978**, *16*, 627.
(25) Fixman, M.; Skolnick, J. *Macromolecules* **1978**, *11*, 863.
(26) Reed, C. E.; Reed, W. F. *J. Chem. Phys.* **1990**, *92*, 6916.
(27) Li, X.; Reed, W. F. *J. Chem. Phys.* **1991**, *94*, 4568.
(28) Miller, G. B. M.S. Thesis, Tulane University, 1992.
(29) Podgornik, R.; Rau, D. C.; Parsegian, V. A. *Macromolecules* **1984**, *17*, 4, 1780.
(30) Tinland, B.; Rinaudo, M. *Macromolecules* **1989**, *22*, 1863.
(31) Tong, Y.; Ghosh, S.; Reed, W. F. Unpublished results.
(32) Ghosh, S.; Peitzsch, R. M.; Reed, W. F. *Biopolymers* **1992**, *32*, 1105.
(33) O'Donnell, G. W.; Richards, G. N. *Aust. J. Chem.* **1973**, *26*, 2041.
(34) Lai, Y. Z.; Ontto, D. E. *Carbohydrate Res.* **1979**, *75*, 51.
(35) Gasman, R. C.; Johnson, D. C. *J. Org. Chem.* **1966**, *31*, 1830.
(36) Piszkiewicz, D.; Bruice, T. C. *J. Am. Chem. Soc.* **1967**, *89* (24), 6237.
(37) Bo, S.; Milas, M.; Rinaudo, M. *Int. J. Biol. Macromol.* **1987**, *9*, 153.
(38) Gravanis, G.; Milas, M.; Rinaudo, M.; Clarke, A. J. *Int. J. Biol. Macromol.* **1990**, *12*, 195.